HiSST: 2nd International Conference on
High-Speed Vehicle Science & Technology
11–15 September 2022, Bruges, Belgium

IXV Flight Rebuilding

Martin SPEL[1], *Eddy CONSTANT*[1], *Valentin MONTEILLET*[1], *Jean-Pierre TRIBOT*[2]

Abstract

R.Tech develops its own CFD software MISTRAL since 2004. The code MISTRAL is composed of several modules, of which MISTRAL-CFD is of interest for the current study. MISTRAL-CFD is a chemical and thermal non-equilibrium Navier-Stokes solver. The code has been used and validated in a large number of French and European projects [1].
Recently, R.Tech develops the coupling between MISTRAL to solve the hypersonic flow and OpenFoam to compute the heat transfer through the structure. A first validation of the coupling has been achieved in [2] , by comparing the thermal evolution in a honeycomb structure placed in a hypersonic wind tunnel.
As part of its validation to address re-entry issues, the purpose of the associated paper is to present the rebuilding using MISTRAL CFD coupled to OpenFoam thermal solver (chtMultiregionFoam [3]) on the IXV flight which provides extremely valuable data for code validation purposes. This study is a first approach to CFD/heat transfer coupling validation with MISTRAL on a real re-entry flight case which set the basis of a high-fidelity multi-physical tool gathering CFD, material behavior and degradation in the future.
A study on the modeling effects has been performed, showing that the most important modeling aspect remains the catalycity model. A modification of a standard atmosphere model by reconstructing atmospheric density show a really good fit with the flight data. Transient heat conduction studies have been performed showing the importance of applying a couples CFD-transient heat transfer approach for this kind of study.

Keywords: *Hypersonic Flow, Heat Transfer, Flight Rebuilding, IXV, Atmospheric model*

Nomenclature

Latin

CFD – Computational Dynamics
$DSMC$ – Direct Simulation Monte Carlo
A_N – Normal Acceleration
C_N – Normal Aerodynamic Coefficient
m – Mass of the vehicle
S_{ref} – reference surfaces
V – Velocity of the vehicle
C_p – Material heat capacity
h – Enthalpy
h_S – Enthalpy at stagnation point
Q – Heat Flux
T – Temperature in the material
T_∞ – Temperature of atmosphere

Greek

κ – Material conductivity
ρ – Air density

1. Introduction

In the frame of national and international space law regulations, a large number of tools has been developed in order to treat the complexity of the physical processes involved in an atmosphere re-entry of vehicles and debris. Nevertheless, important uncertainties in re-entry physics remains due to the lack of data and knowledge to calibrate our model. Then the interest of developing more complex codes with coupled physics, such as coupling CFD and thermal analysis makes perfect sense. Within the framework of the improvement/validation of MISTRAL and the in-depth understanding of the re-entry process, data from experiments is essential.

[1] *R.Tech, Parc Technologique Delta Sud, 09340, Verniolle, France, martin.spel@rtech.fr*
[2] *DASSAULT AVIATION, 78, quai Marcel Dassault Cedex 300, 92552 SAINT-CLOUD CEDEX, France,jean-pierre.tribot@dassault-aviation.com*

On 11 February 2015, the IXV conducted its first 100-minute space flight, successfully completing its mission upon landing intact on the surface of the Pacific Ocean. The IXV separated from the Vega launcher and begun its reentry at 120 km altitude, traveling at a recorded speed of 7.5 km/s, identically to a typical re-entry path of a low Earth orbit (LEO) spacecraft.

The objective of this paper is to challenge the code MISTRAL (a CFD software developed at R.Tech) on the IXV flight rebuilding and to set the basis of CFD/thermal coupling in order to achieve in the future more complex studies with this software.

The first part of the paper present a brief overview of all experimental probe which provide the flight data to validate the simulations, the tools and the meshes used to perform numerical simulations. The second part of the paper will focus on the study of different models of catalycity, transport models and kinetic models to see which are most suitable for simulating real flight conditions. They were carried out on three precise points of the trajectory, taking as a reference an atmosphere model as input parameter. The third part will be devoted to calculations on the entire trajectory with the complete geometry. The objective is to rebuild the flow densities from the normal force acceleration and reconstruct an atmospheric model. The last part focuses on a transient thermal analysis through the coupling of MISTRAL and OpenFOAM software to study the thermal inertia effects, using the derived densities, and concentrating on the structure heating.

2. Set up

2.1. Probe Location

Two types of sensors has been used on the IXV vehicle, pressure probes and thermocouples. These are defined by a number and two letters, which correspond respectively to their location, nose, base, flap, leeward, hinge panel, cavity and windward, and their type (see Fig. 1) .

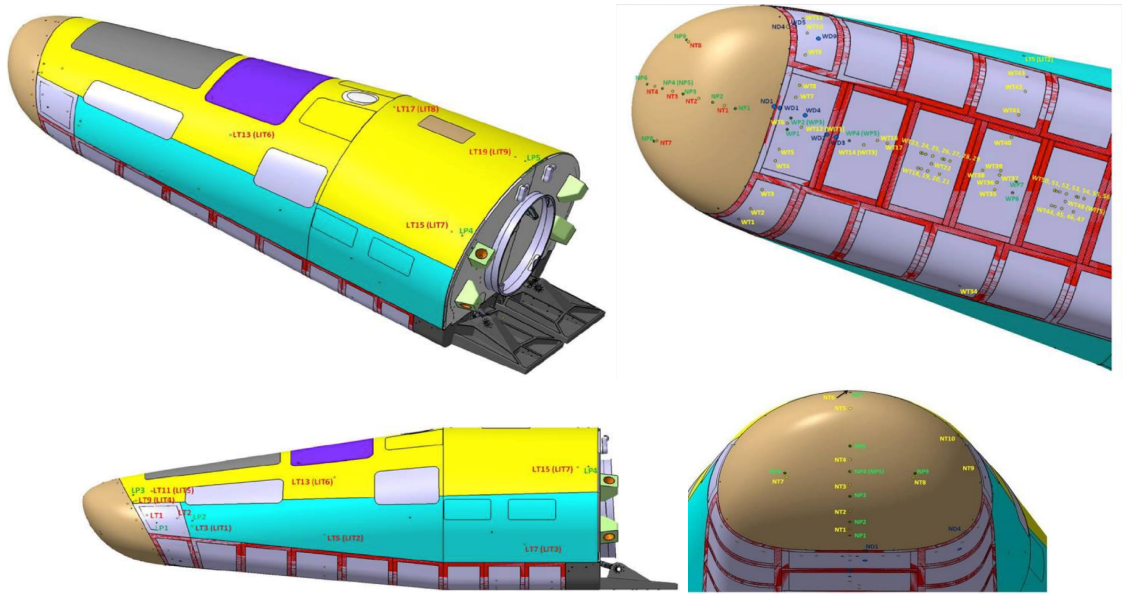

Fig 1. Leeward, Nose, Side, Windward Area

For convenient reasons of comparisons between CFD and real flight, the data will be compared on some probes picked on the nose and the windward to get local comparisons and on the symmetry line (Fig. 2) to get the comparison on the global behavior of the flow.

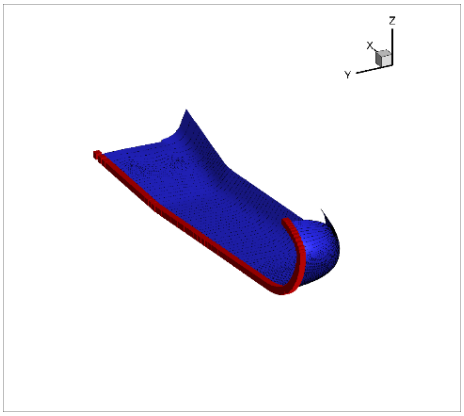

Fig 2. Symmetry Line

2.2. Software used for the reconstruction

2.2.1. MISTRAL

The CFD calculations are made with MISTRAL-CFD, a code developed by RTech, which is a Navier-Stokes numerical code applicable in the continuum domain. It was designed for atmospheric re-entry calculations with a highly parallel approach. A Van Leer-AUSM hybrid scheme is used. The resolution of the system of equations is carried out by the GMRES implicit method. The second order solver is achieved using the MUSCL extrapolation, with a reduction to the first order in the shock regions by limiters. In the current set of computations the MinMod limiter is used. For the high-speed re-entry where the real gas modeling is important, the equilibrium or non-equilibrium chemistry model can be activated.

2.2.2. OpenFoam

OpenFoam is a free, open source software released and developed since 2004. The open source toolbox provides an efficient coding and a suitable environment for the implementation and the rapid dissemination of new algorithms to the users community, with the target to be used further to investigate real industrial problems. The code OpenFoam has been used by R.Tech for several CNES studies for both CFD and thermodynamics analysis [2]. The heat transfer solver, detailed in [3] has been widely used for thermal reconstruction.

2.2.3. GridPro

GridPro is a high-quality grid generator which permits automated multi-block structured grid generation featuring orthogonality, smoothness and robustness. GridPro is widely used in different domains like turbo machinery, Oil and Gas, Aerospace etc.

2.3. Mesh

The GridPro software has been used to create the meshes used in the present studies for both MISTRAL and OpenFoam Solvers.

2.3.1. CFD Mesh of the full geometry

MISTRAL uses block structured hexagonal grid cells. Here, two grid levels are used with 11972 blocks each (see Fig. 2). The first cell height is fixed at $1.0e^{-6}$ m. The number of cells associated with each mesh is shown in the Table 1.

Table 1. Number of cells around the complete geometry

Mesh	Number of cells
Coarse	224 368
Medium	1 794 944

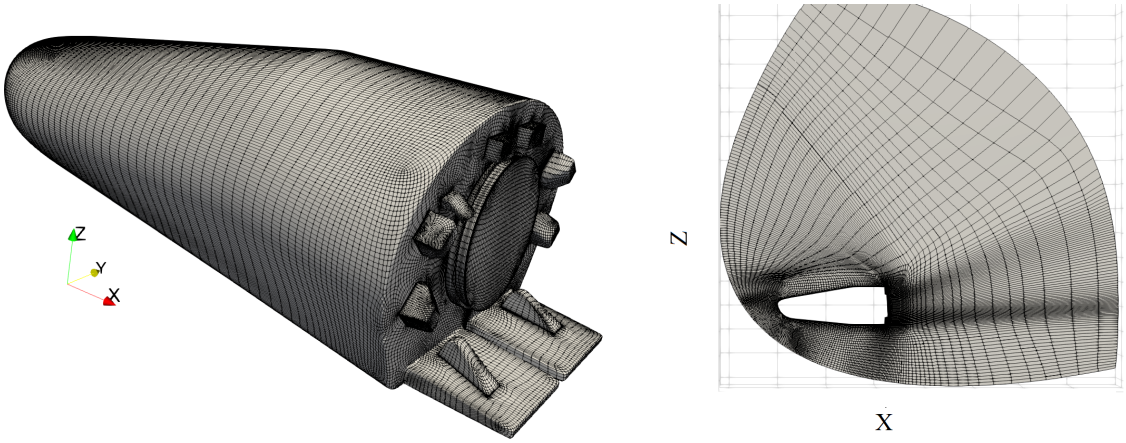

Fig 3. Medium mesh of the IXV geometry

2.3.2. CFD Mesh of the fore-body geometry

In order to accelerate the computation, a mesh has been generated also on the fore-body as the all field is not always needed in the present study. Here, three grid levels are used with 995 blocks each (shown Fig. 4). The first cell height is fixed at $1.0e^{-6}$ m. The number of cells associated with each mesh is shown in the Table 2.

Table 2. Number of cells for the fore-body mesh

Mesh	Number of cells
Coarse	39 872
Medium	318 976
Fine	2 551 808

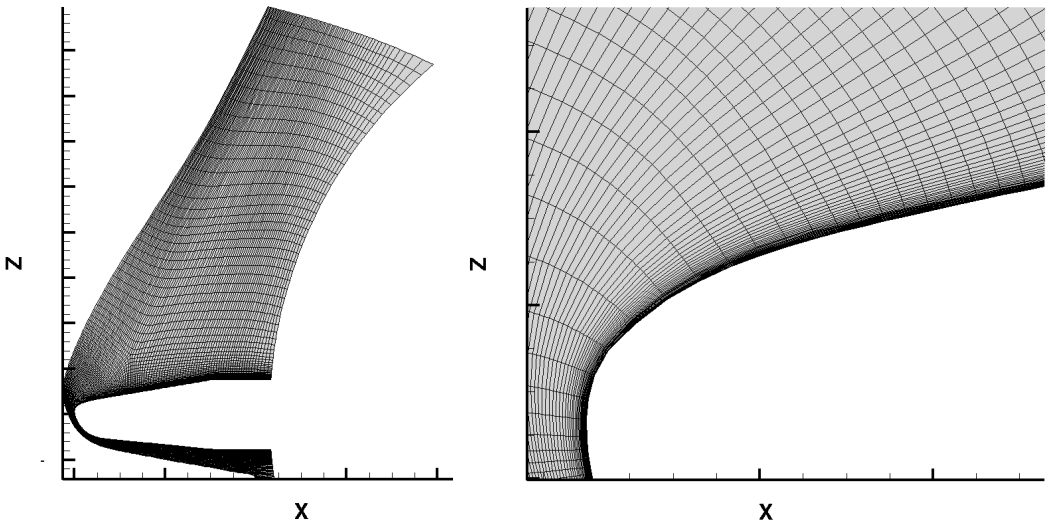

Fig 4. Fine Mesh of the IXV fore-body

2.3.3. Transient Heat Mesh

The mesh used to compute the transient heat was generated by extrusion of the MISTRAL surface fore-body mesh presented Fig. 5. The simulation has been performed on a coarse and medium mesh of the fore-body. The number of cells used in each mesh are presented in Table 3

Table 3. Number of cells for the transient heat mesh

Mesh	Number of cells
Coarse	120 000
Medium	800 000

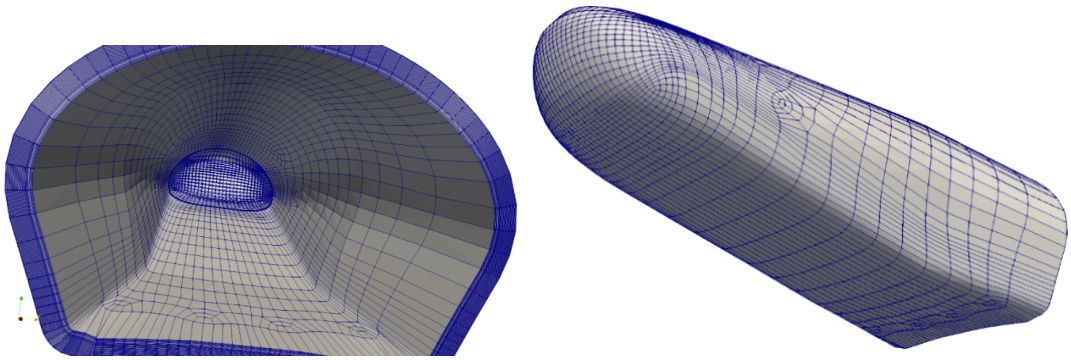

Fig 5. OpenFoam Medium Mesh

3. Modeling sensitivities

The aim of this part is to determine the parameters to use for the reconstruction of the flight. To this end, thirty-six calculations, each on three grid levels (Table 4) have been performed. All these cases ran on the fore-body mesh, in laminar regime on three flight points, chosen as function of their Mach. A radiative equilibrium temperature is used on the wall with an emissivity of 0.8.

Table 4. Flight conditions for local trajectory points

Id	$Mach$	$\rho[kg.m^3]$	$T[K]$	$U[m.s^{-1}]$
1	25	$2.62e^{-5}$	204.59	7169.76
2	20	$1.0e^{-4}$	222.44	5988.19
3	20	$1.31e^{-4}$	226.98	6051.76
4	20	$9.59e^{-5}$	222.44	5988.19
5	17.75	$2.25e^{-4}$	239.60	5508.82

Different densities have been used for the Mach 20 case. The first one (id 2) correspond to a pre-flight trajectory estimation. The second one (id 3) to the MSISE atmosphere model at the altitude of the flight GPS. Finally, some work on density reconstruction has been performed in order to predict a more realistic atmospheric density (id 4).

3.1. Modeling Effect

A first serie of calculations comparing the pseudo-catalytic (imposed mass fraction at the wall) , non-catalytic and the PCD models (the stagnation point scaled VKI catalycity model) has been achieved at different flight points and viscosity models (see Table 5).

Table 5. Modeling Effect

Cases	Id	Catalycity Model	Chemistry Model	Viscosity Model	Mixture Model
1/2	3	Non/pseudo	Dunnkang	Blottner per species	No
3/4	2	Non/pseudo	Dunnkang	Blottner per species	No
5/6	2	Non/pseudo	Dunnkang	Sutherland	No
7/8	2	Non/pseudo	Dunnkang	Sutherland	Yes
9/10/11	2	Non/pseudo	Dunnkang	Sutherland per species	No
22/23/24	1	Non/PCD/pseudo	Dunnkang	Blottner per species	No
32/33/34	5	Non/PCD/pseudo	Dunnkang	Blottner per species	No

The results on the temperatures at the symmetry line (Fig. 2) for non catalytic and pseudo catalytic model is presented Fig. 6. It can be observed that the temperatures recorded on the symmetry line during the flight were permanently between the temperatures estimated by the two extreme catalycity models

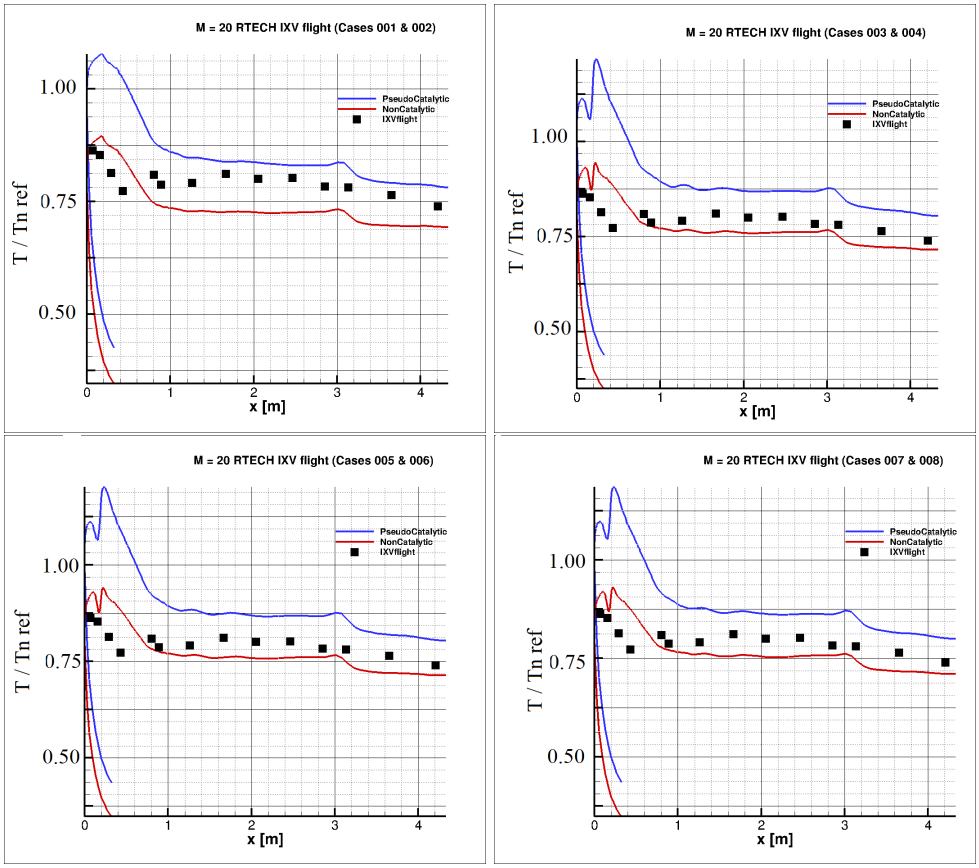

Fig 6. Wall temperature at symmetry line

The Fig. 7 shows the comparisons between the PCD, catalytic and non catalytic models. It can be seen that PCD model, in between the 2 other models, gives already good results as soon as one moves away from the nose of the vehicles.

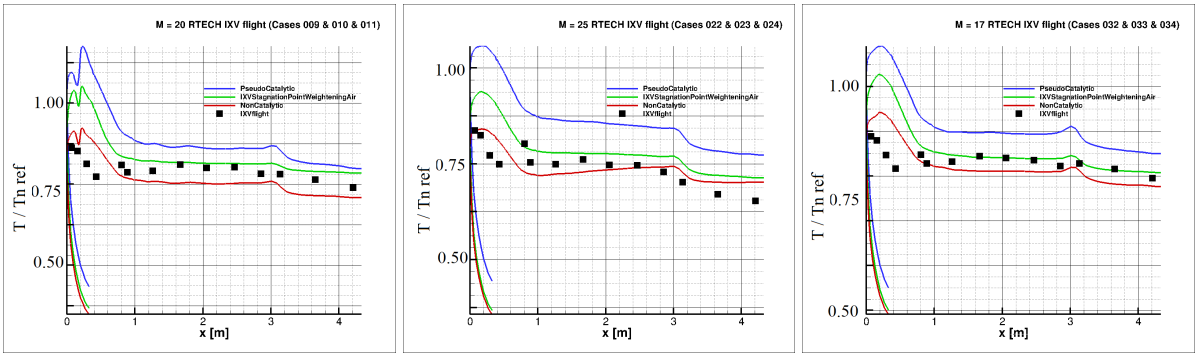

Fig 7. Wall temperature on symmetry line with PCD catalycity model

The PCD being developed for the IXV project is supposed to be the most realistic model and gives promising results on the temperature together with the non catalytic model. Thus both will be chosen for the rest of the calculation.

3.2. Viscosity Model Effect

The following set of test cases presented Table 6 compare the viscosity models at different flight points.

Table 6. Viscosity Effect

Cases	Id	Catalycity Model	Chemistry Model	Viscosity Model	Mixture Model
14/15	4	PCD	Dunnkang	Sutherland per species	No
16/19	2	PCD	Dunnkang	(Blottner/GuptaYos per species)	No

The Fig. 8 shows that the viscosity models give similar results, with temperatures relatively close to those of the experimental models for comparison of the Sutherland and Blottner models, especially for the case with the reconstructed atmospheric density (id 4).

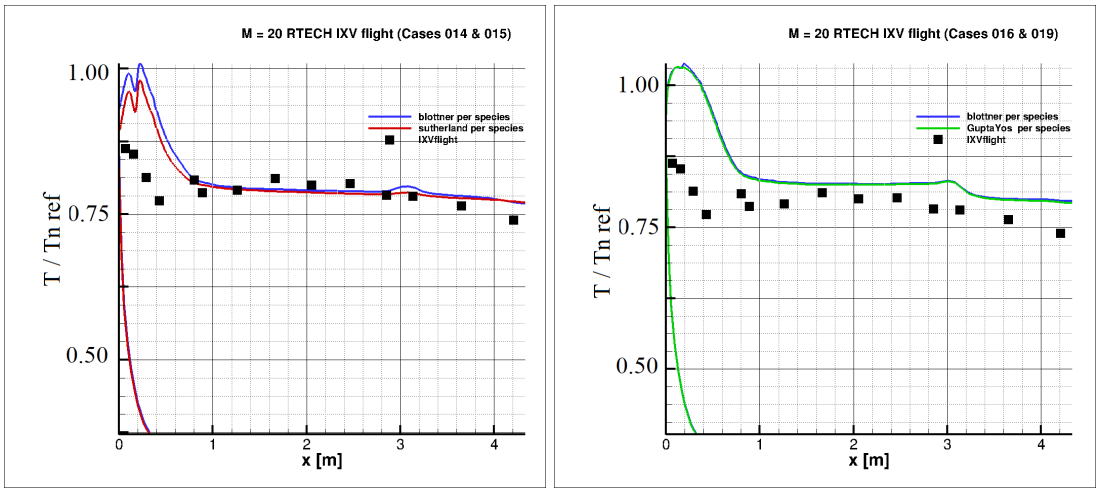

Fig 8. Wall temperature at symmetry line. Viscosity Effect

The baseline viscosity model was Blottner for the per species velocities, combined with Wilke. The Sutherland species viscosity model has been implemented for comparison. While the diffusive fluxes

are higher for the Sutherland model than for the Blottner model, the overall heating rate is not changing considerably as shown Fig. 9.

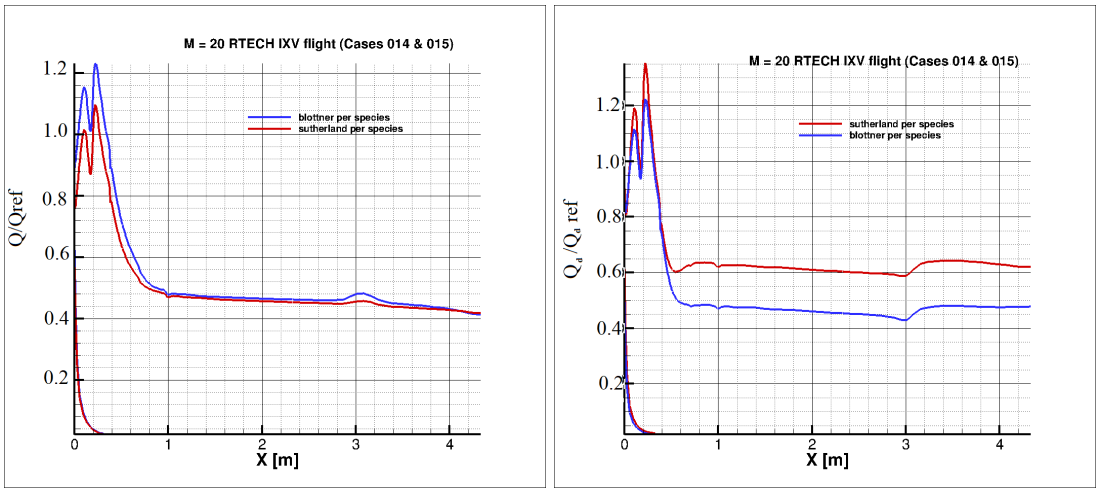

Fig 9. Total and diffusive heat flux on symmetry line (Sutherland/Blottner)

Between the Gupta-Yos model and the Blottner shown Fig. 10 model hardly any changes are observed.

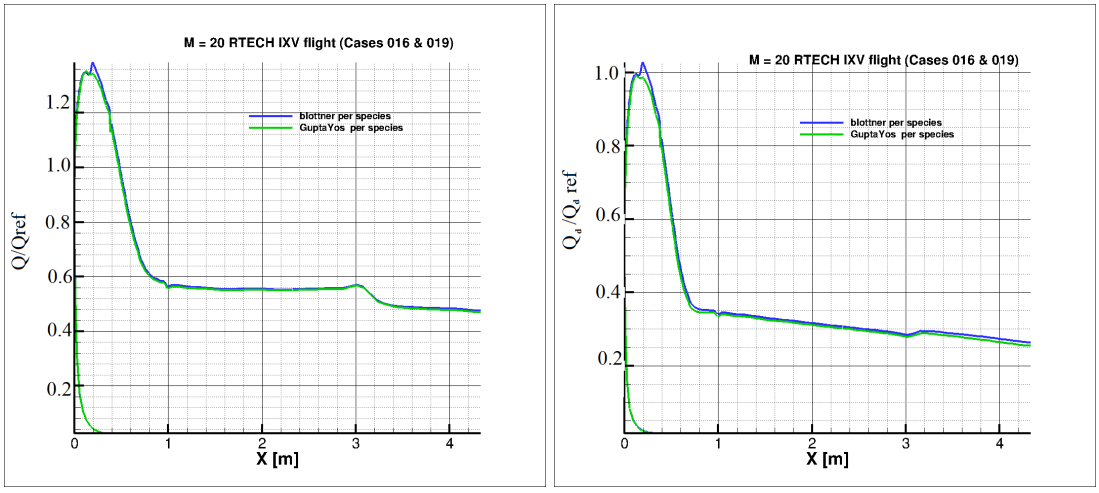

Fig 10. total and diffusive heat flux on symmetry line (Blottner/Gupta Yos)

3.3. Chemistry Model Effect

To study the chemistry effect, PCD and Blottner were taken as the catalicity model and the viscosity model respectively. The Dunn-Kang chemistry model was replaced by both a 10 species and 5 species Park model (cases 16,17 and 18), and a three-temperature model has been also evaluated. The cases conditions tested are gathered in Table 7.

The Fig. 11 shows that the different chemical models predict similar temperatures, while slightly overestimating the experimental values (using the MSISE atmospheric densities).

Table 7. Chemistry Effect

Cases	Id	Catalycity Model	Chemistry Model	Viscosity Model	Mixture Model
16/17/18	2	PCD	Dunnkang/Park93-(10/5) species	Blottner per species	No
16/50	2	PCD	Dunnkang/Dunnkang3Tv	Blottner per species	No

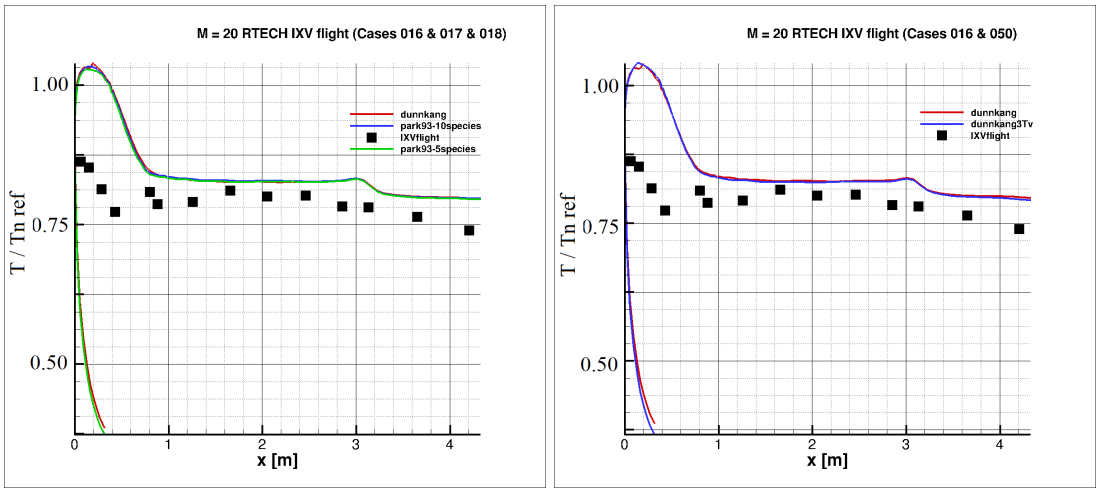

Fig 11. total and diffusive heat flux on symmetry line (Blottner/Gupta Yos)

The total and chemical flows of the different models are also really close (Fig. 12& 13).

As a conclusion, the choice of chemical model has not much influence on the results for the flight conditions selected.

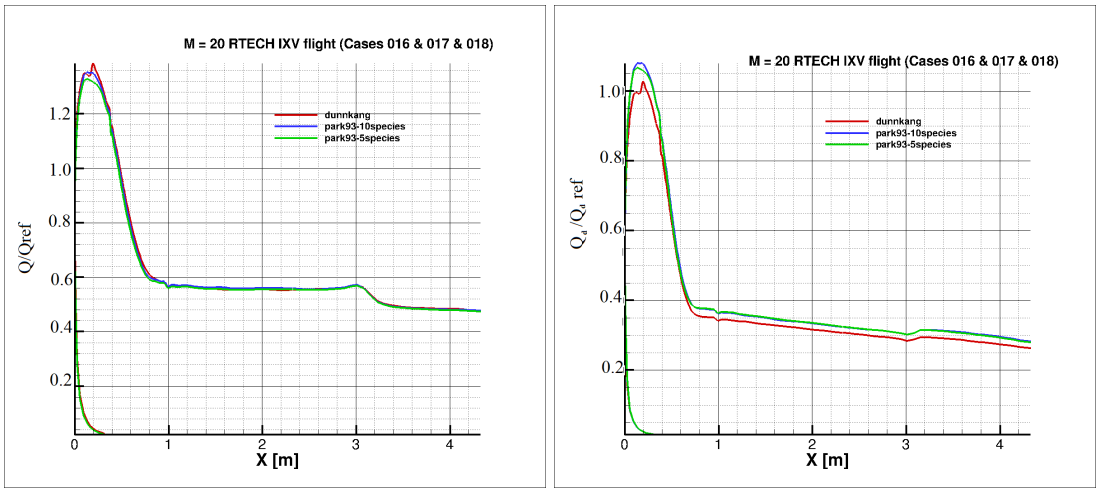

Fig 12. total and diffusive heat flux on symmetry line (Dunnkang/Park93-5species/Park93-10species)

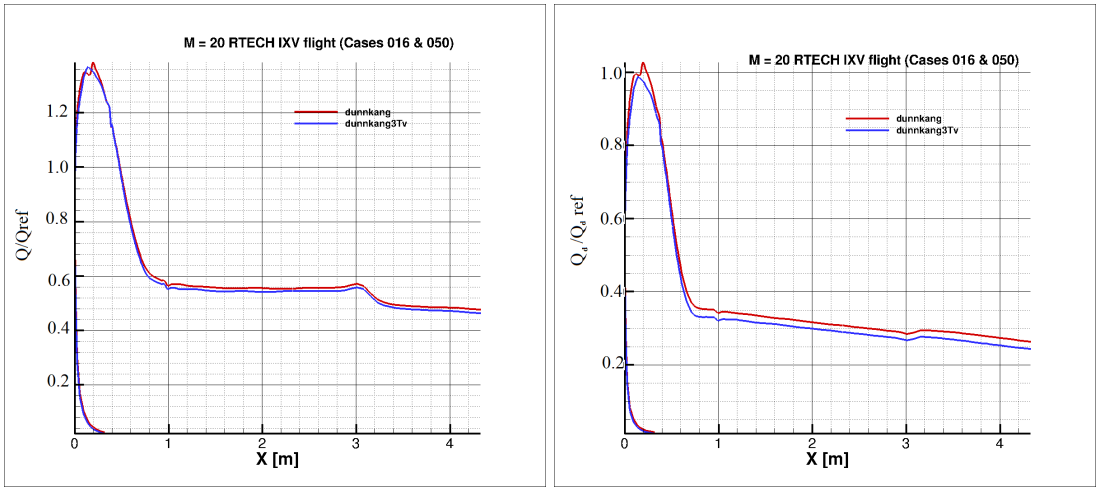

Fig 13. total and diffusive heat flux on symmetry line (Dunnkang/Dunnkang3Tv)

4. Complete Trajectory Computations

The purpose of this section is to simulate the entire vehicle re-entry phase and compare the results with the flight data. The calculations presented below take into consideration the conclusions made in the previous section. The Blottner species viscosity model, Dunn-Kang kinetics and the PCD model were taken as baseline models of viscosity, chemistry and catalycity. A radiative equilibrium temperature is used on the wall with an emissivity of 0.8.

4.1. Atmosphere model for input parameter

Fig. 14 shows the pressure on the symmetry line for 3 flight positions (shown Table 4) with the fore-body mesh. We observed significant differences for the pressures between CFD results with density atmosphere model and IXV flight data.

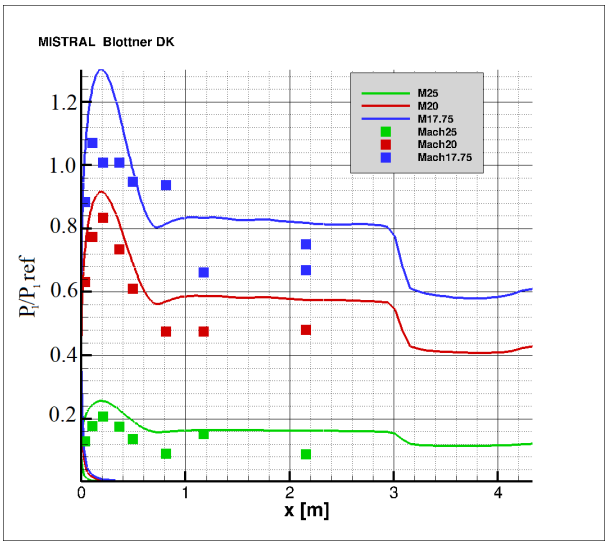

Fig 14. Comparison between CFD and IXV flight data

It is known that the surface pressure is generally predicted quite accurately by CFD computations. These results therefore suggest that the atmosphere model on which the calculations are based does not allow for a very good fit with the flight data. Complete trajectory calculations on the full geometry (see Fig. 3) have been made in order to confirm the trend observed. The results are presented for several

probes Fig. 15. These discrepancies are confirmed when comparing the values of pressure probe by probe.

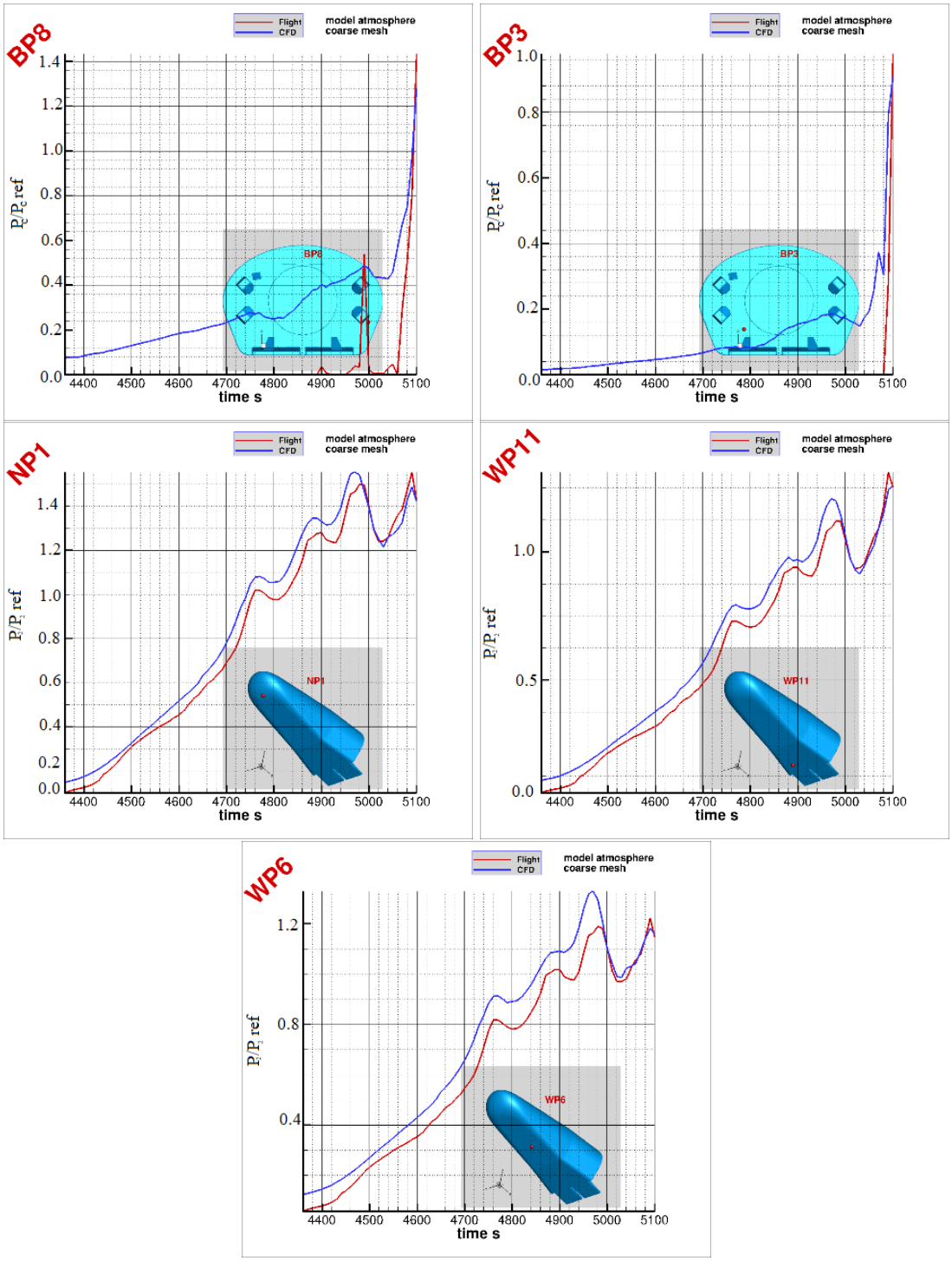

Fig 15. Comparison of pressure (Atmospheric model/IXV flight data)

The aim is now to know if it is possible to obtain by another means a density closer to the one encountered in real conditions.

4.2. Flight density reconstruction

Based on [4], the formula Eq. 1 allows to deduce the density starting from the normal force coefficient:

$$\rho_{C_N} = \frac{A_N.m}{\frac{1}{2}.V^2.S_{REF}.C_N} \tag{1}$$

where :

- A_N is the normal acceleration
- V the velocity
- $S_{REF} = 7.26m^2$ the reference surface
- C_N the normal aerodynamic coefficient
- m the mass of the vehicle

By extracting C_N based on S_{REF} from CFD of the full geometry and measured normal acceleration from atmosphere model calculations (see Fig. 16), we obtain a new density which will serve as an input parameter for future calculations.

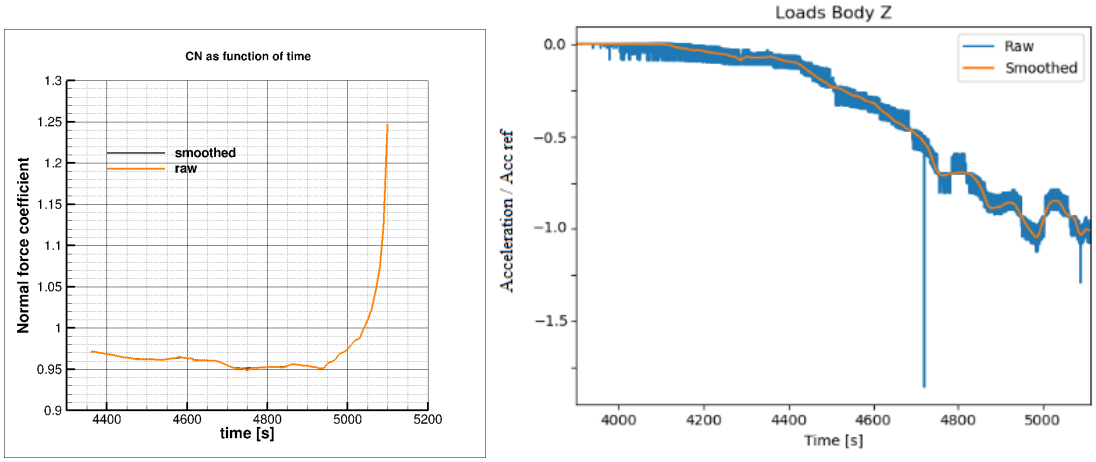

Fig 16. Raw and smoothed data of CN and normal acceleration for the calculation with atmospheric model density

In order to be able to reproduce the entire IXV re-entry trajectory , 121 calculations were performed each 10 s of the flight. From the results, a new density was determined for each case using Eq. 1. The normal loads from flight data have been filtered in order to get a smooth variation of the reconstructed density (orange line on right side of Fig. 16). Fig. 17 shows the comparison between the MSISE model densities and the derived flight densities.

After deriving the new densities, new computations on the fore-body mesh were performed with the updated atmospheric densities. The Fig. 18, on the front body geometry, shows that once the density is corrected, on the symmetry line, pressure computed are closer to those measured in flight.

Calculations on the complete trajectory for the full geometry have been performed then with the new densities and is presented Fig. 19 & 20. The results shows a good agreement with the flight data (with pressure curves almost overlapping) which validate the methodology for the atmospheric density correction.

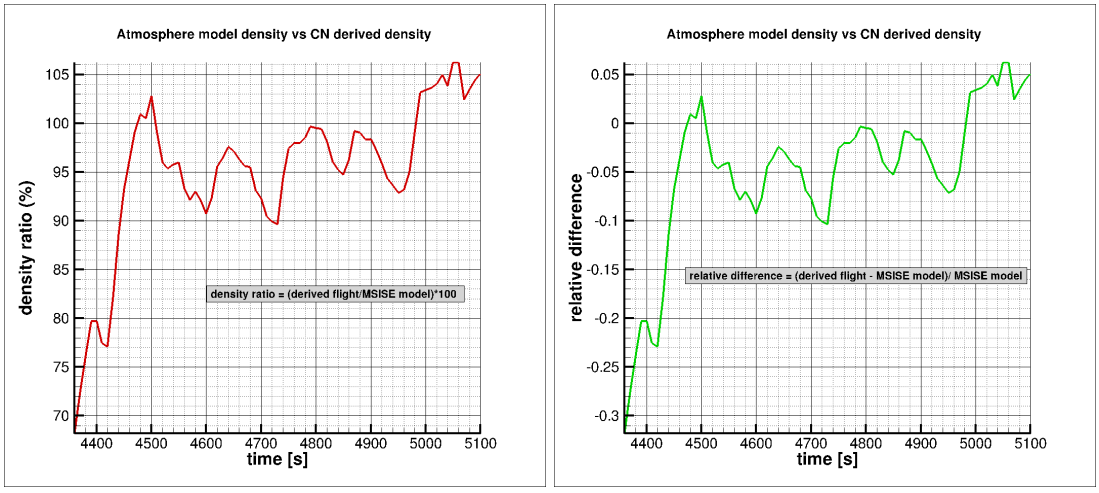

Fig 17. Density ratio and relative difference between old and new density

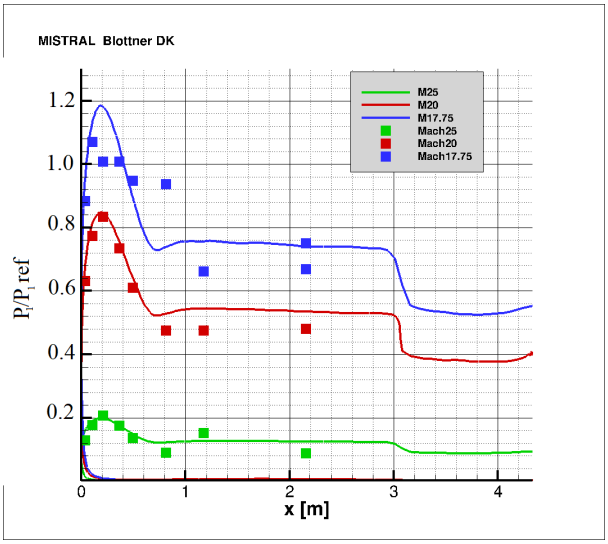

Fig 18. Comparison between CFD and IXV flight data (corrected density)

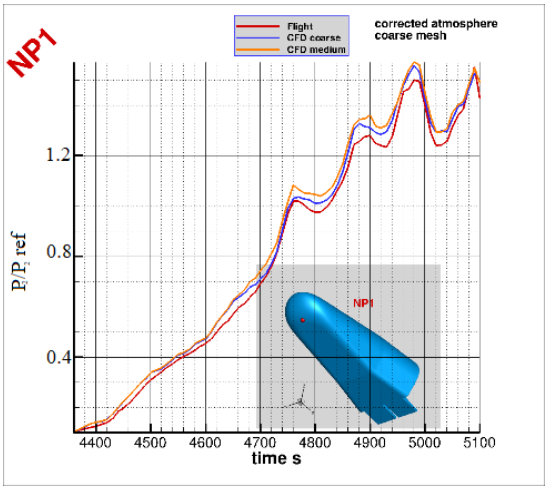

Fig 19. Comparison of pressure on the nose (NP1)(Corrected density/IXV flight data)

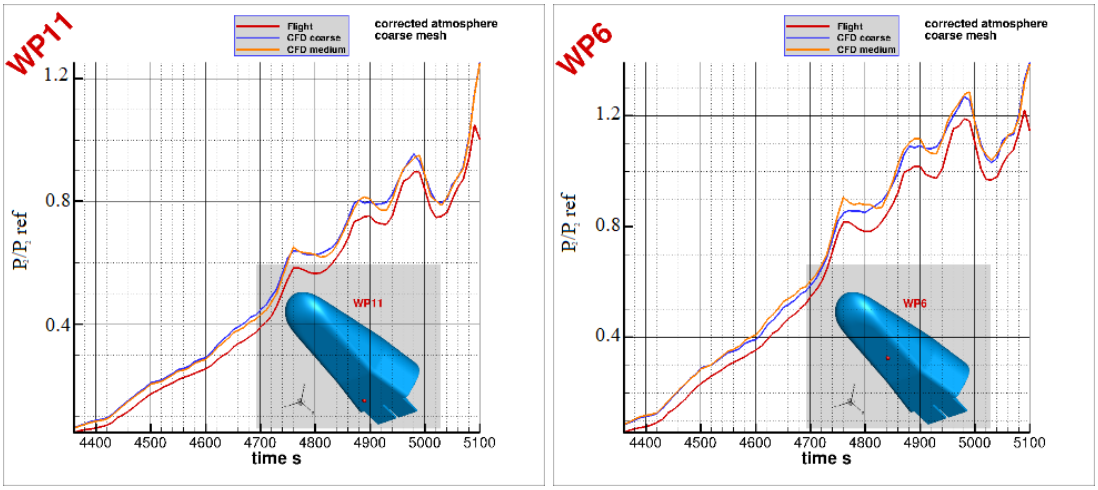

Fig 20. Comparison of pressure on the windward (WP6 & WP11) (Corrected density/IXV flight data)

As shown for pressure, the temperature computed at the symmetry line show better agreement with the flight data when using the corrected atmospheric densities. The current approach provide then a better estimation of the atmospheric density than a standard atmosphere model in the continuum regime. An attempt was made to extend the methodology to the transitional and rarefied regimes but due to the fact that only a continuum flow solver has been used, the aerodynamic coefficients was not reliable enough to perform such study. Therefore no density corrections have been applied to these regimes.

5. Transient Heat

5.1. Objectives

As it can been seen in the precedent paragraphs, a discrepancy between the temperatures on the nose-cap has been observed. Even for the non-catalytic model the temperatures are higher than the measurements. In fact physically speaking as far as thermocouples are concerned the trend observed on the nose region is currently unexplained as no boundary layer was observed in flight. One of the possible explanation would be the lake of coating "titanium nitride" able to avoid platinum sheath of thermocouple type S to react with Si of the C/SiC of the TPS. Various hypothesis have been proposed, under which the malfunctioning of the nose-cap probes above certain temperatures, and the effect of heat-soak. To study the later effect, a transient thermal analysis has been achieved based on the fluxes predicted by MISTRAL. The study has been performed on the fore-body mesh with OpenFoam transient heat transfer solver.

5.2. CFD

The full time frame from t=3900s to t=5100s has been computed using CFD. The uncertainties in the rarefied and transitional regimes are quite high (pressures, fluxes), but it was found to be better to have slightly wrong fluxes during the continuum phase, than to make estimation on surface temperature starting from t=4370s in the continuous regime as was done in the first attempts. The current approach could be extended with DSMC computations. R.Tech has equally developed the MISTRAL-DSMC code, but which does not take into account the chemistry yet. Since the chemistry could play a major role in the heating, improvements to MISTRAL-DSMC should be made before applying it.

5.3. Transient heat Solver and coupling strategy

The thermal solver chtMultiregionFoam of OpenFoam has been used:

- The energy equation is solved through the solid :

$$\frac{\partial \rho h}{\partial t} = \frac{\partial}{\partial x}\left(\frac{\kappa}{C_p}\frac{\partial h}{\partial x}\right) \tag{2}$$

- The flux imposed at the wall is coming from MISTRAL solver corrected by a hot wall correction based on the inflow properties which read:

$$Q(T) = \frac{h_S - C_{p_{air}}(T)T}{h_S - C_{p_{air}}(T_\infty)T_\infty} Q_{MISTRAL} \tag{3}$$

- This technique has been validated with TSAGI experiments on a honeycomb plate structure at Mach 14 for the heat transfer analysis (detailed in [2])

The algorithm reads:

1. Start run at t=3900s.
2. Get normalized heating map from MISTRAL at time t
3. Interpolate on the OpenFoam surface mesh
4. Advance the heating at 10 seconds, using the local flow conditions Q, and the farfield conditions to compute the hot wall correction
5. Go back to step 2

5.4. Results

The full trajectory has been computed with both the PCD model and the non-catalytic model. In the Fig 21, & 22 below the results on different probes are shown for the non catalytic model on the left, and for the PCD model on the right. Excellent grid convergence is observed, meaning that already on a mesh with around 50.000 cells reasonable heat fluxes are obtained.

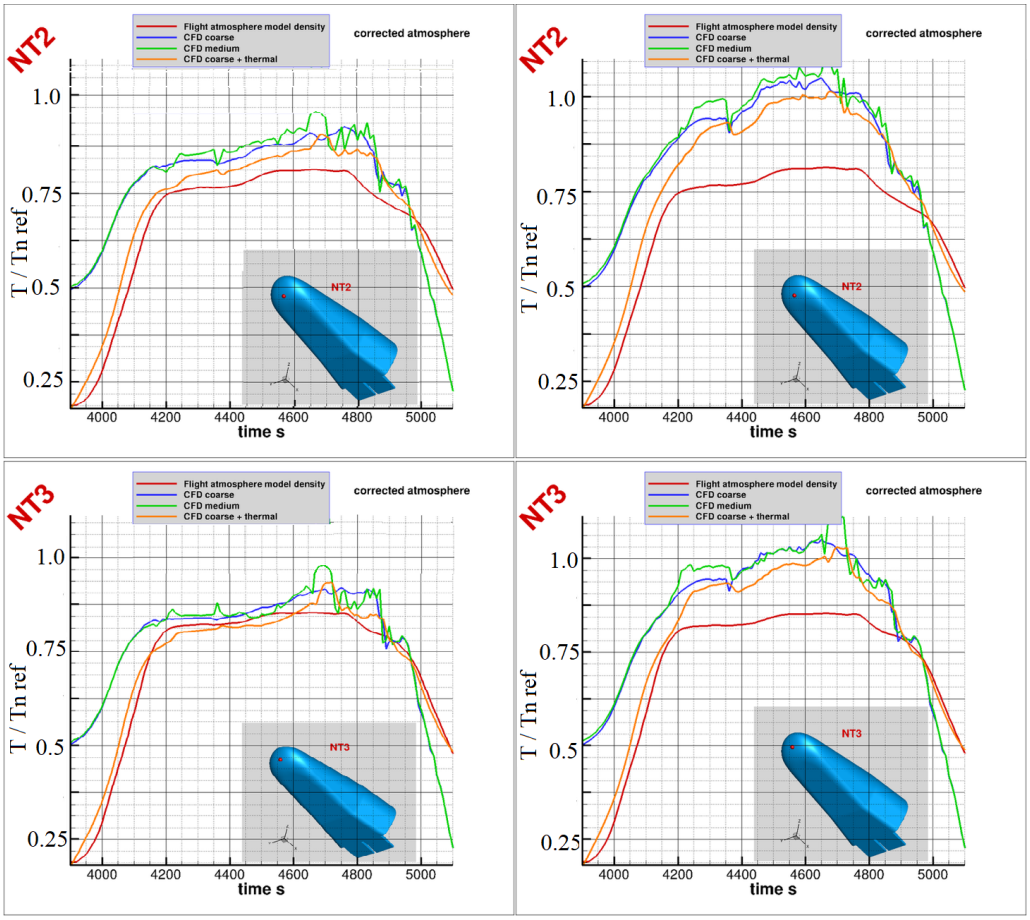

Fig 21. Temperature at probe on nose over time. Non catalytic model (left), PCD model (right)

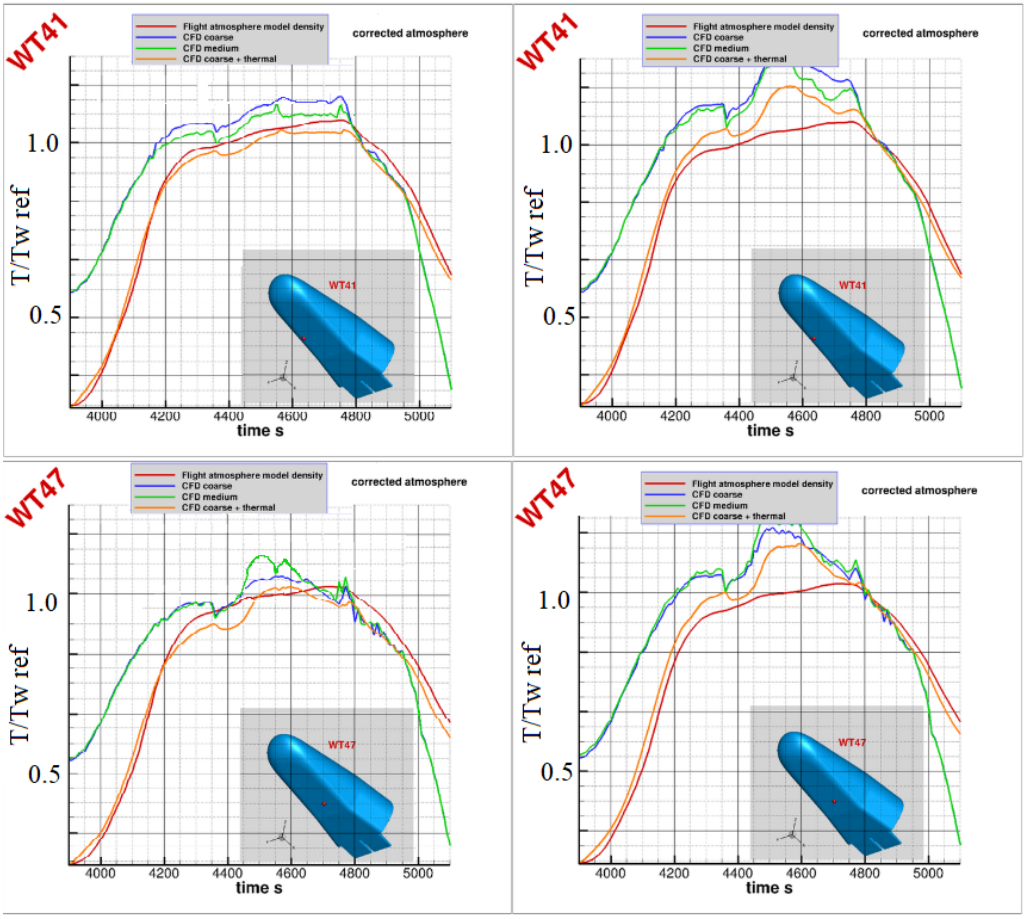

Fig 22. Temperature at probe on windward over time. Non catalytic model (left), PCD model (right)

6. Conclusion

The IXV flight provides extremely valuable data for code validation purposes.

An extensive study on modeling sensitivity and flight rebuilding has been performed over a one-year period. Some new viscosity models have been implemented in MISTRAL during this study which strengthens the code in the position of one of the industry references in Europe.

On the other hand a considerable in-kind contribution has been made in order to provide a better predictions of the wall pressures and wall temperatures.

A study on the modeling effects has been performed, showing that the most important modeling aspect remains the catalycity model. The study on the reconstruction of the atmospheric density, requiring full body 3D computations along the full trajectory, has provided promising results. As this study has only been performed in the continuum regime, it could be extended to the transitional regime by using MISTRAL-DSMC in future works. Transient heat conduction studies have been performed in order to examine the heat-soak effects. As it can be seen, large difference are observed in both the heating and the cooling phase, showing the importance of applying a couples CFD-transient heat transfer approach for this kind of study. It is demonstrated that the TPS CMC material used for IXV flight was smoothly catalytic. Additional effort to be done for characterizing properly and accurately the TPS CMC material.

Further effort will be made on to upgrade the spacecraft oriented object PAMPERO [5], to perform the same kind of calculations and compare the results

Acknowledgment

This work was supported by the ESA through the IXV and Space Rider projects. RTech thanks the help of Thales Alenia Space and Dassault Aviation for the realization of this project

References

[1] J. Tribot, S. Dutheil, P. Viguier, J. Verant, D. Charbonnier, J. Vos, P. Van-Hauwaert, M. Spel, D. F. V. Mareschi, and G. Rufolo, "Intermediate experimental vehicle extrapolation ground to flight wind tunnel and cfd approach," in *64th International Astronautical Congress*, (Beijing, China), 2013.

[2] J. Annaloro, V. Ledermann, E. Constant, M. Spel, C. Vasse, V. Rivola, S. Dozdov, and P. Omaly, "Rebuilding with pampero of destructive hypersonic tests on honeycomb sandwich panels in the t-117 wind tunnel," in *10th IAASS conference*, (Los Angeles, USA), 2019.

[3] M. E. Abbassi, D. Lahaye, and C. Vuik, "Modelling turbulent combustion coupled with conjugate heat transfer in openfoam," in *MCS 10 Tenth Mediterranean Combustion Symposium, Reports of the Delft Institute of Applied Mathematics*, vol. 17-11, (Naples, Italy), 2017.

[4] J. T. Findlay, G. M. K. Patrick, and A. Troutman, "Final report - shuttle derived atmospheric density model part 2: Sts atmospheric implications for aotv trajectory analysis - a proposed gram perturbation density model," tech. rep., NASA, 1984. NASA Contractor Report 171824.

[5] J. Annaloro, S. Galera, P. Kärräng, Y. Prévereaud, J.-L. Vérant, M. Spel, P. V. Hauwaert, and P. Omaly, "Space debris atmospheric entry prediction with spacecraft-oriented tools," in *7th European Conference on Space Debris*, 2017.